Chapter 2
Introduction to Solar Cell Operation

This chapter discusses the very fundamental working principle of a solar cell. It is intended to briefly motivate the relevance of carrier recombination and carrier transport to solar cell operation without going into technological detail.

2.1 Doped Semiconductors

2.1.1 The Band Gap

An adequate description of electrons in a crystal (represented by a periodic assembly of atoms) would require the solution of a many-electron problem with a Hamiltonian involving both the interaction between electrons and atomic nuclei as well as the interaction among electrons. However, in order to qualitatively motivate some fundamental properties of metals and semiconductors, it may suffice to focus on weakly bound electrons (Bloch electrons) in an effective one-electron potential representing the interaction with a matrix of atomic nuclei.[1] For all Bravais lattice vectors $\mathbf{R}$ of the crystal lattice, the potential $\mathcal{U}(\mathbf{r})$ must obey

$$\mathcal{U}(\mathbf{r}+\mathbf{R}) = \mathcal{U}(\mathbf{r}). \tag{2.1}$$

Bloch's theorem states that for such a periodic effective one-electron potential $\mathcal{U}(\mathbf{r})$, the eigenstates $\psi_{\mathbf{k}}$, which are solutions of the Schrödinger equation

$$\left(-\frac{\hbar^2}{2m}\nabla^2 + \mathcal{U}(\mathbf{r})\right)\psi_{\mathbf{k}}(\mathbf{r}) = \varepsilon_{\mathbf{k}}\psi_{\mathbf{k}}(\mathbf{r}) \tag{2.2}$$

---

[1] The main lines of reasoning in this section draw on full derivations given in [1].

J. Giesecke, *Quantitative Recombination and Transport Properties in Silicon from Dynamic Luminescence*, Springer Theses, DOI: 10.1007/978-3-319-06157-3_2,
© Springer International Publishing Switzerland 2014

to eigenvalues $\varepsilon_{\mathbf{k}}$, can be chosen as the product of a plane wave and a function $u_{\mathbf{k}}(\mathbf{r})$ with the periodicity of the Bravais lattice

$$\psi_{\mathbf{k}}(\mathbf{r}) = e^{i\mathbf{k}\cdot\mathbf{r}} u_{\mathbf{k}}(\mathbf{r}). \tag{2.3}$$

With reciprocal lattice vectors $\mathbf{K}$, the periodicity of the Bravais lattice allows expression of the eigenstates $\psi_{\mathbf{k}}$ and the potential $\mathcal{U}(\mathbf{r})$ in terms of Fourier components $c_{\mathbf{k}-\mathbf{K}}$ and $\mathcal{U}_{\mathbf{K}}$ as

$$\psi_{\mathbf{k}}(\mathbf{r}) = \sum_{\mathbf{K}} c_{\mathbf{k}-\mathbf{K}} e^{i(\mathbf{k}-\mathbf{K})\cdot\mathbf{r}} \tag{2.4}$$

$$\mathcal{U}(\mathbf{r}) = \sum_{\mathbf{K}} \mathcal{U}_{\mathbf{K}} e^{i\mathbf{K}\cdot\mathbf{r}}. \tag{2.5}$$

In the limit of vanishing $\mathcal{U}_{\mathbf{K}}$, insertion of this expression for $\psi_{\mathbf{k}}$ into Eq. 2.2 reveals a parabolic electron band structure with degenerate eigenvalues at Bragg planes (Brillouin zone boundaries). For a weak but finite $\mathcal{U}_{\mathbf{K}}$, perturbation theory yields a splitting of otherwise degenerate energy levels at a magnitude of $2 \cdot |\mathcal{U}_{\mathbf{K}}|$ [1]. This finding implies a vanishing density of electronic states at certain energy levels.

According to the Pauli exclusion principle, the ground state of a gas of weakly bound Bloch electrons (valence electrons) in a crystalline solid implies occupation of all one-electron levels below a so-called Fermi energy ε_F, which is distinguished by requiring the total number of one-electron levels with energies less than ε_F to be equal to the number of Bloch electrons in a crystalline solid [1]. The Pauli exclusion principle is also reflected in the Fermi-Dirac distribution representing the occupation probability

$$f(\varepsilon_{\mathbf{k}}) = \frac{1}{e^{\frac{\varepsilon_{\mathbf{k}}-\varepsilon_F}{k_B T}} + 1} \tag{2.6}$$

of free (or quasi-free) one-electron levels. If—for reasons outlined above—there is a considerable difference between the highest occupied level and the lowest unoccupied level in the ground state of the electron gas (at temperature $T = 0$), this energy difference is referred to as a *band gap*. Adjacent bands are denoted as valence band (below the band gap) and conduction band (above the band gap).

2.1.2 Classification of Semiconductors

Both electronic and optical properties of crystalline solids are essentially affected by the existence and width of a band gap and by the characteristics of the band structure near the band gap. Insulating solids are distinguished by a band gap much greater than $k_B T$. Intrinsic semiconductors feature a band gap in the range of $k_B T$, whereas metals

feature a vanishing band gap. The above perception of the term semiconductor [1] is somewhat inadequate with regard to most semiconductors of technological relevance (e.g. for silicon, the band gap is more than 40 times greater than room temperature $k_B T$). Therefore, here the term semiconductor shall denote crystalline solids with a band gap in the energy range of visible light.

2.1.3 Interaction with Light—Indirect Semiconductors

Electrons in solids may interact with photons. Such optical transitions enable excitation of electrons from their ground state to a previously unoccupied state. The interaction between light and matter must obey conservation of energy, momentum, and angular momentum. For indirect semiconductors such as silicon and germanium, the locations of conduction band minimum and valence band maximum in $\mathbf{k}$-space differ such that the interaction between electrons and photons must involve another excitation (e.g. a phonon) in order to satisfy conservation of momentum. The characteristic of an indirect semiconductor largely affects the optical properties of silicon, as the prerequisite of excitation or anihilation of phonons renders both absorption of light as well as radiative recombination very unlikely compared to a direct semiconductor of comparable band gap. This fact is essential when relating recombination lifetime as inferred from measurements of radiative recombination (luminescence) to other recombination causes such as scattering of electrons at impurities and crystal defects.

2.1.4 Doping

In a semiconductor with n_v valence electrons per atom, adding atoms with $n_v \pm 1$ valence electrons induces shallow electronic states in the band gap. Such states are much confined ($\sim k_B T$) to an energy range close to the conduction band edge for $n_v + 1$ (donors, n-type doping, e.g. phosphorous doping of silicon) whereas they are much confined to an energy range close to the valence band edge for $n_v - 1$ (acceptors, p-type doping, e.g. boron doping of silicon).

Adding of donors (free electrons) or acceptors (free vacancies or *holes*) to a semiconductor brings about a significant change of electrical conductivity, which can be explained by a high degree of room temperature ionization of the electronic states induced via doping—or in other words by a high free carrier concentration. Acceptor levels allow thermal excitation of electrons from the adjacent valence band, whereas donor electrons are easily thermally excited into the adjacent conduction band.

With a density of electronic states per energy and volume in a solid $D(\varepsilon_{\mathbf{k}})$, the dark densities of electrons and holes are

$$n_e^0 = \int_{\varepsilon_C}^{\infty} d\varepsilon_{\mathbf{k}}\, f(\varepsilon_{\mathbf{k}}) D(\varepsilon_{\mathbf{k}}) \tag{2.7}$$

$$n_h^0 = \int_{-\infty}^{\varepsilon_V} d\varepsilon_{\mathbf{k}} \left[1 - f(\varepsilon_{\mathbf{k}})\right] D(\varepsilon_{\mathbf{k}}). \tag{2.8}$$

Here, ε_C and ε_V denote edges of the conduction and valence band, respectively. For a symmetric shape of $D(\varepsilon_{\mathbf{k}})$ with respect to the band gap (intrinsic semiconductor), this implies a Fermi energy close to the center of the band gap, leading to an intrinsic free carrier concentration in silicon of $n_i \approx 10^{10}\,\mathrm{cm}^{-3}$ at room temperature [2–5]. However, with a substantial amount of electronic states near either conduction band or valence band, the symmetry of $D(\varepsilon_{\mathbf{k}})$ is destroyed, leading to a shift of Fermi energy toward the respective band edge in order to satisfy Eqs. 2.7 and 2.8. For $T = 0$, the Fermi energy must lie between the respective band edge and the adjacent energy level of the donors or acceptors—leading to a vanishing concentration of free carriers. Yet, at an increasing temperature the Fermi level advances toward the center of the bandgap, such that at room temperature free carrier concentration (ionized dopant concentration) nearly corresponds to dopant concentration. At typical dopant concentrations of 10^{15}–$10^{16}\,\mathrm{cm}^{-3}$ this brings about an increase of free carrier density and hence of electrical conductivity by 5–6 orders of magnitude.

The density of free carriers due to ionized dopant atoms is denoted as majority carrier density, whereas the density of the complementary charge carrier species is denoted as minority carrier density. The shift of Fermi energy in a doped semiconductor away from the minority carrier band leads to an inverse proportionality between dark minority carrier density and dopant concentration.

2.2 Quasi-Fermi Energy—Electrochemical Potential

While the band population via free electrons (and—equivalently—holes) may be described via Fermi-Dirac statistics according to Eq. 2.7, this description is complicated in the presence of additional generation of excess carrier density Δn beyond dark equilibrium. The concept of so-called Quasi Fermi levels aims at an adequate description of such a state of electrochemical non-equilibrium.

2.2.1 Quasi-Fermi Levels

Due to a square root shape of the density of states $D(\varepsilon_{\mathbf{k}}) \propto \sqrt{\pm\left(\varepsilon_{\mathbf{k}} - \varepsilon_{C/V}\right)}$, free carrier densities in the dark may be accurately expressed as[2]

$$n_e^0 = N_C e^{\frac{\varepsilon_F - \varepsilon_C}{k_B T}}, \tag{2.9}$$

$$n_h^0 = N_V e^{\frac{\varepsilon_V - \varepsilon_F}{k_B T}}, \tag{2.10}$$

with N_C and N_V denoting effective densities of states of the conduction and valence band

$$N_C = 2\left(\frac{2\pi m_e^* k_B T}{h^2}\right)^{\frac{3}{2}}, \tag{2.11}$$

$$N_V = 2\left(\frac{2\pi m_h^* k_B T}{h^2}\right)^{\frac{3}{2}}, \tag{2.12}$$

and with effective masses of electrons and holes [1] $m_{e/h}^*$ and the Planck constant h.

In the case of excess carrier generation beyond thermal equilibrium, the population of valence and conduction band through excess carriers is no longer adequately described via Fermi-Dirac statistics. Whereas in the dark state, the product of minority and majority carrier densities must correspond to intrinsic carrier density $n_e^0 n_h^0 = n_i^2$, now both carrier species feature enhanced densities, requiring a shift of Fermi energy toward both band edges. This dilemma is resolved by the concept of quasi-Fermi energies, which allow the description of a state of electrochemical non-equilibrium of a semiconductor under illumination via Fermi-Dirac statistics. Quasi-Fermi energies ε_{FC} and ε_{FV} of electrons and holes replace Fermi energy ε_F in the Fermi-Dirac distribution (cf. Eq. 2.6), respectively. Electron and hole densities can thus be expressed as[3]

$$n_e = n_e^0 + \Delta n = N_C e^{\frac{\varepsilon_{FC} - \varepsilon_C}{k_B T}}, \tag{2.13}$$

$$n_h = n_h^0 + \Delta n = N_V e^{\frac{\varepsilon_V - \varepsilon_{FV}}{k_B T}}. \tag{2.14}$$

The separation of quasi-Fermi energies of electrons and holes relates to the implied voltage U of a semiconductor under illumination $\varepsilon_{FC} - \varepsilon_{FV} = qU$. The following derivation reveals the relation between quasi-Fermi levels and the so-called electrochemical potential of carriers.

---

[2] This approximation is deemed accurate for $|\varepsilon_F - \varepsilon_{C/V}| \gtrsim 3k_B T$.

[3] Here, $\Delta n_e = \Delta n_h = \Delta n$ is assumed.

2.2.2 The Electrochemical Potential

The change of internal energy dE of a statistical ensemble such as a gas of electrons or holes corresponds to the balance of changes of all relevant energy forms[4]

$$dE = TdS^T - pdV + \mu_c dN + \phi dQ. \tag{2.15}$$

Here, changes of thermal energy, compressional energy, chemical energy, and electrical energy are considered. The system is distinguished by the intensive variables temperature T, pressure p, chemical potential μ_c, and electrical potential ϕ. Further, the extensive variables giving rise to a change of internal energy are the entropy S^T, the volume V, the particle number N, and the charge Q. The energy which a solar cell delivers to a load is given by the sum of the changes of free energy $dF_{e/h}$ of electrons and holes, respectively.

$$dF = dE - d\left(TS^T\right) = S^T dT - pdV + \mu_c dN + \phi dQ \tag{2.16}$$

With constant semiconductor volume and temperature during solar cell operation, this expression simplifies accordingly such that

$$dF = (\eta_e + \eta_h)\, dN, \tag{2.17}$$

with the electrochemical potential

$$\eta_{e/h} = \mu_{c,e/h} \mp q\phi, \tag{2.18}$$

and with the positive elementary charge q. With a free energy increment according to Eq. 2.17, the electrochemical potential represents the essential potential of excess carriers in semiconductors. Its gradient gives rise to net currents of excess carriers.

Consider the mean energy per particle of a gas of $N_{e/h}$ free electrons/holes at temperature T

$$\langle \varepsilon_{e/h} \rangle = \pm \varepsilon_{C/V} + \frac{3}{2} k_B T = \frac{TS^T_{e/h} + p_{e/h}V + \eta_{e/h}}{N_{e/h}}. \tag{2.19}$$

Making use of the modified Sackur-Tetrode equation expressing the entropy of an ideal gas [6]

$$S^T_{e/h} = k_B N_{e/h} \left(\frac{5}{2} + \ln \frac{N_{C/V}}{n_{e/h}} \right) \tag{2.20}$$

and exploiting the equation of state of an ideal gas

[4] This derivation proceeds along the lines of a derivation given in [6].

$$p_{e/h}V = N_{e/h}k_BT, \tag{2.21}$$

one obtains

$$n_e = N_C e^{\frac{\eta_e - \varepsilon_C}{k_BT}}, \tag{2.22}$$

$$n_h = N_V e^{\frac{\eta_h + \varepsilon_V}{k_BT}}. \tag{2.23}$$

Comparison to Eqs. 2.13 and 2.14 reveals

$$\eta_e = \varepsilon_{FC} \tag{2.24}$$

$$\eta_h = -\varepsilon_{FV}. \tag{2.25}$$

Therefore, the implied voltage U of a semiconductor under illumination can be expressed via the sum of electrochemical potentials

$$qU = \varepsilon_{FC} - \varepsilon_{FV} = \eta_e + \eta_h = \eta_\sum. \tag{2.26}$$

With a chemical potential of the form

$$\mu_{c,e/h} = k_BT \ln \frac{n_{e/h}}{a_{e/h}} \tag{2.27}$$

with constant densities $a_{e/h}$,[5] according to Eq. 2.18 the electrochemical equilibrium condition (vanishing separation of quasi-Fermi energies $\eta_\sum = 0$) yields

$$a_e a_h = n_e^0 n_h^0 = n_i^2. \tag{2.28}$$

Consequently, the separation of quasi-Fermi energies $\eta_\sum$ can be expressed in terms of the product of minority and majority carrier density as

$$\eta_\sum = k_BT \ln \frac{n_e n_h}{n_i^2}. \tag{2.29}$$

2.3 The pn-Junction

The essential task of a photovoltaic device is to separate electrical charge released upon absorption of light—preferrably at the highest possible conversion efficiency from photon energy to electrical energy (as the product of voltage and electrical charge). This essential task requires efficient mechanisms of both light absorption

[5] $a_{e/h}$ enable a dimensionless logarithmic argument and incorporate a constant offset of $\mu_{c,e/h}$.

and charge separation. In semiconductor photovoltaic devices, this task is commonly accomplished by a pn-junction within an absorber. This is the interface region between n- and p-doped semiconductor volumes. The light absorbing semiconductor bulk supplies electrical charge, while the pn-junction provides a means to separate it.

The charge current released by an illuminated pn-junction device with a separation of quasi-Fermi energies $qU = \eta_{\sum}$ gives rise to the delivery of work to an external load. In the following, this charge current is motivated—substantiating the relevance of transport properties such as carrier mobilities, diffusion coefficients, and dopant concentrations.

2.3.1 Dark pn-Junction

Electron and hole charge current density in semiconductors can be expressed in terms of the gradient of the electrochemical potential. With the electrical conductivity

$$\sigma_{e/h} = q n_{e/h} \mu_{e/h} \tag{2.30}$$

and with $\mu_{e/h}$ denoting electron and hole carrier mobilities, electron or hole charge current density is

$$\mathbf{j}_{Q,e/h} = \pm \frac{\sigma_{e/h}}{q} \nabla \eta_{e/h}. \tag{2.31}$$

Insertion of the electrochemical potential of Eq. 2.18 with a chemical potential given by Eq. 2.27 yields charge currents

$$\mathbf{j}_{Q,e/h} = \pm \frac{\sigma_{e/h}}{q} \left(\frac{k_B T}{n_{e/h}} \nabla n_{e/h} \pm q\mathbf{E} \right), \tag{2.32}$$

with a local electrical field $\mathbf{E} = -\nabla\phi$. In the dark, i.e. in electrochemical equilibrium, net current must vanish everywhere in the semiconductor, which is equivalent to the condition

$$\frac{k_B T}{n_{e/h}} \nabla n_{e/h} = \pm q\mathbf{E}. \tag{2.33}$$

Thus, in dark equilibrium, the gradient of electron and hole densities must be balanced by a local electrical field. Integrating Eq. 2.32 across the pn-junction from the n-contact to the p-contact (indicated via superscript here) yields

$$\phi^n_{e/h} - \phi^p_{e/h} = \pm \frac{k_B T}{q} \ln \frac{n^n_{e/h}}{n^p_{e/h}}. \tag{2.34}$$

The quantity $\phi^n_{e/h} - \phi^p_{e/h}$—which is also referred to as a dark diffusion voltage [6]—accounts for the compensation of electrical and chemical potential differences across the pn-junction such that in electrochemical equilibrium the voltage between the terminals of a (dark) pn-junction device is zero.

The large difference between free electron and hole densities across the pn-junction leads to diffusion of carriers from the region where they represent majority carriers to the region where they represent minority carriers. This diffusion process brings about a buildup of local charge within a so-called space charge region.

2.3.2 Illuminated pn-Junction

Illumination of a pn-junction with photon energies above the band gap leads to band-to-band photon absorption and generation of excess charge carrier density Δn. This process increases the number of free electrons and holes by the same amount. Dark majority and minority carrier concentrations commonly differ by a factor of

$$\frac{n^0_{maj}}{n^0_{min}} = \left(\frac{n^0_{maj}}{n_i}\right)^2 \ggg 1. \tag{2.35}$$

Therefore, the relative increase of minority carrier concentration upon illumination is much greater than the relative increase of majority carrier concentration, and the space charge and the diffusion voltage of the pn-junction are substantially reduced as a consequence of excess carrier generation—as can already be concluded from Eq. 2.34.

$$\left|\phi^n_{e/h} - \phi^p_{e/h}\right|_{\Delta n=0} > \left|\phi^n_{e/h} - \phi^p_{e/h}\right|_{\Delta n>0} \tag{2.36}$$

In the metal contacts of a pn-junction, there is no band gap and therefore excess carrier density must smoothly approach zero toward the terminals at the side faces of a pn-junction. This again implies that the difference of chemical potentials between the terminals of a pn-junction must not change upon excess carrier generation

$$\left|\ln n^n_{e/h} - \ln n^p_{e/h}\right|_{\Delta n=0} = \left|\ln n^n_{e/h} - \ln n^p_{e/h}\right|_{\Delta n>0}. \tag{2.37}$$

Thus, the voltage delivered at the metal electrodes of an illuminated pn-junction corresponds to the amount by which the diffusion voltage of the pn-junction (cf. Eq. 2.34) is reduced through a finite excess carrier density. This state of electrochemical non-equilibrium is equivalent to a finite separation of quasi-Fermi energies $0 \neq \eta_{\sum} = qU$. Figure 2.1 depicts the space charge, the band edges, and the quasi-Fermi levels of electrons and holes in a pn-junction device both, in (dark) electrochemical equilibrium, and under illumination or carrier injection.

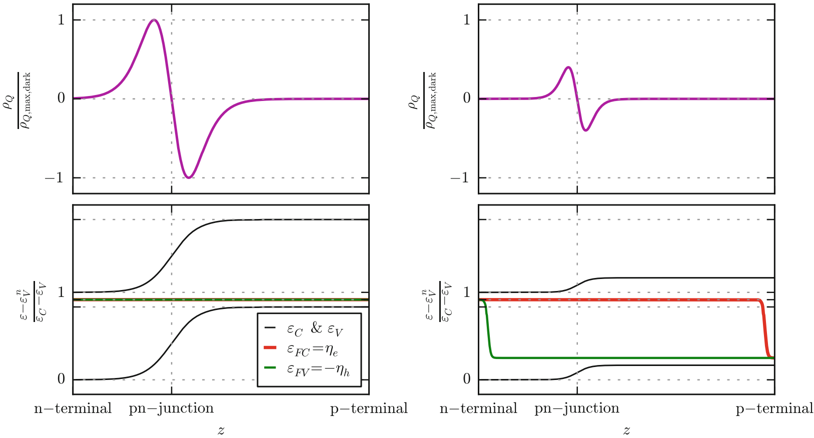

Fig. 2.1 Depiction of local charge density ρ_Q, valence and conduction band edges, and the quasi-Fermi energies (± electrochemical potentials) of electrons and holes across a pn-junction. The state of electrochemical equilibrium without illumination (*left*) is compared to the non-equilibrium state under illumination—featuring a finite separation of quasi-Fermi energies $\eta_{\sum} = qU$ corresponding to the implied voltage U. ε_V^n denotes the energy of the valence band edge at the *n*-terminal

2.3.3 Charge Current of a pn-Junction

As yet, the implied voltage of a pn-junction device under illumination has been motivated. However, what has not been motivated so far is the nature of the charge current out of the pn-junction device, which gives rise to the delivery of work in an external load. With electrical conductivity as specified in Eq. 2.30 and along the lines of Eq. 2.31, the total charge current density in a pn-junction device corresponds to the sum of charge current densities of electrons and holes

$$\mathbf{j}_Q = \frac{1}{q}\sum_{e/h} \pm\sigma_{e/h}\nabla\eta_{e/h}. \tag{2.38}$$

The charge current released at the terminals of a pn-junction device is a majority carrier drift current. As such, the solar cell current is induced by an electrical field—albeit not explicitly by the field of the space charge region, which does not deliver work on carriers [6]. In order to motivate the driftlike characteristic of a solar cell current, the nature of drift and dielectric relaxation has to be reflected upon. As one may conclude from Eqs. 2.17 and 2.18, minimization of free energy in a solar cell is equivalent to minimization of the sum of chemical potentials (via diffusion/random motion) and of electrical potentials (via field-driven drift/dielectric relaxation) of charge carriers, respectively.

2.3.3.1 Dielectric Relaxation

Considering the dissipation of a local charge density ρ_Q, the combination of the conservation of charge[6]

$$\frac{\partial \rho_Q}{\partial t} + \nabla \mathbf{j}_Q = 0 \tag{2.39}$$

with the charge current density

$$\mathbf{j}_Q = \sigma \mathbf{E} \tag{2.40}$$

and with the differential representation of Gauss's law

$$\epsilon \epsilon_0 \nabla \mathbf{E} = \rho_Q \tag{2.41}$$

yields the ordinary equation

$$\left(\frac{d}{dt} + \frac{\sigma}{\epsilon \epsilon_0} \right) \rho_Q = 0. \tag{2.42}$$

Its solution for an initial value $\rho_Q(t = 0) = \rho_{Q,0}$ and with a dielectric relaxation time $\tau_{diel} = \frac{\epsilon \epsilon_0}{\sigma}$ is

$$\rho_Q(t) = \rho_{Q,0} e^{-\frac{t}{\tau_{diel}}}. \tag{2.43}$$

With electrical conductivity as of Eq. 2.30, τ_{diel} must be much shorter for majority carriers than for minority carriers. Therefore, local charge imbalances in doped (and nondegenerate) semiconductors dissipate via dielectric relaxation of majority carriers. With the dielectric constant of silicon $\epsilon \approx 12$, the vacuum permittivity [4] $\epsilon_0 = 8.854 \times 10^{-14}\,\mathrm{A\,s\,V^{-1}\,cm^{-1}}$, a carrier mobility of roughly $\mu \approx 10^3\,\mathrm{cm^2\,V^{-1}\,s^{-1}}$, and the elementary charge $q = 1.602 \times 10^{-19}\,\mathrm{A\,s}$, τ_{diel} may be roughly approximated as

$$\tau_{diel} \approx \frac{7 \times 10^3}{n_{maj}}\,\mathrm{cm^{-3}s}, \tag{2.44}$$

which is below the range of picoseconds for typical dopant concentrations (e.g. $\tau_{diel} \approx 5 \times 10^{-13}$ s for 1 Ω cm p-type material). Within this timescale, the characteristic travelling distance of drift-induced transport can be conservatively estimated by solar cell thickness ($d \approx 2 \times 10^{-2}$ cm). Comparison with carrier diffusion distances within this timescale of typically $\sqrt{D\tau_{diel}} \lesssim 5 \times 10^{-6}\,\mathrm{cm} \ll d$ (diffusion coefficient D) allow the conclusion that drift and dielectric relaxation of local excess charge

[6] Derivation proceeds along the lines of [6].

proceeds instantaneously on relevant timescales of carrier diffusion through the solar cell. This justifies the assumption of local quasi charge neutrality $\Delta n = \Delta n_e \approx \Delta n_h$ outside the space charge region.

2.3.3.2 Diffusion Currents

Let us assume constant dopant concentrations $n^0_{e/h}$ on both sides of a pn-junction such that $\nabla n_{e/h} = \nabla \Delta n$ holds locally, and let the chemical potential drop due to changes of electron and hole concentration across the pn-junction be entirely compensated by an inverse electrical potential drop in the space charge region. Let us further assume a vanishing electrical potential gradient beyond the space charge region—i.e. vanishing majority carrier drift. In this hypothetical scenario, any gradient of the electrochemical potential would have to be due to a gradient of excess carrier density, and any electrical current would have to be caused by diffusion. With the assumptions stated above, and accounting for electrical conductivity according to Eq. 2.30, Eq. 2.31 would then become

$$\mathbf{j}_{Q,e/h} = \pm k_B T \mu_{e/h} \nabla \Delta n. \tag{2.45}$$

Consequently, (with $\nabla \Delta n_e \approx \nabla \Delta n_h$) the sum of charge current densities of electrons and holes would have to locally compensate (except for the minor difference between their mobilities). Thus, diffusion currents from the pn-junction to the device terminals do not give rise to a charge release at the terminals of a pn-junction device. Diffusion currents can be detrimental as recombination currents associated with recombination in the bulk and interfaces of an absorber, and at the same time they are vital for solar cell operation as they ensure minority carrier transport to the pn-junction. However, diffusion currents alone cannot explain solar cell operation. Rather, it is a majority carrier drift induced by an electrical potential gradient, which gives rise to charge release at the terminals of a pn-junction device.

2.3.3.3 Selectivity of the pn-Junction

The capability of the pn-junction to actually separate the charge of excess carriers is denoted here as *selectivity*. Two essential features account for the selectivity of a pn-junction: the electrical field of the space charge region, and the large difference between majority and minority carrier conductivities.

The electrical field of the space charge region enables substantial carrier transport against a very pronounced chemical potential gradient. Such net carrier transport is essentially rendered energetically favorable due to elastic backscattering of majority carriers in the space charge region's field. Optical generation of excess carriers then causes a considerable pressure of highly conductive excess majority carriers (and of their corresponding charge) at the device electrodes, respectively. In spite of the relatively high chemical potential of excess majority carriers, this pressure cannot

relax via diffusion across the pn-junction, as this is prevented by the electrical field. Conversely, when connecting the electrodes of an illuminated solar cell via a load, the excess majority carrier charge pressure may relax through this external circuit. Thus, the resulting majority carrier *drift* current is eventually driven by a faint electrical potential gradient due to the connection of the device electrodes via a load. It appears noteworthy that, although the electrical field of the space charge region does not deliver work on charge carriers, it is nonetheless an electrical field which drives—or rather pulls—majority carrier currents out of the electrodes of a solar cell: this is the electrical field established between the electrodes or terminals of a solar cell by connecting them through a load—sustained and fed by the steady-state generation of excess carriers.

2.3.3.4 Drift or Diffusion

As outlined above, solar cell operation is enabled by the interplay of drift and diffusion currents. While the kinetics of transport of minority carriers to the pn-junction is governed by their random motion with a diffusion coefficient D, the kinetics of the transport of majority carriers to the terminals of a photovoltaic device is governed by drift or dielectric relaxation. Both carrier mobilities $\mu_{e/h}$ and concentrations $n_{e/h}$ are crucial determinants of this transport process.

2.4 Solar Cell Efficiency—Loss Mechanisms

The efficiency η of photovoltaic energy conversion is defined as the ratio

$$\eta = \frac{P_{el}}{P_{ph}} \tag{2.46}$$

between the electrical power $P_{el} = U_{mpp} I_{mpp}$ delivered to a load by a photovoltaic device and the light power P_{ph} to which the latter is exposed. Here, U_{mpp} and I_{mpp} denote the steady-state (maximum-power-point) operation voltage and current delivered by a photovoltaic device.

2.4.1 Idealized Reversible Conversion Process

Photovoltaic energy conversion efficiency is inherently costrained to $\eta < 1$, as follows from thermodynamic considerations. An idealized treatment by Landsberg [7, 8] considers the internal energy, the entropy, and the radiation pressure of isotropic blackbody radiation of temperature T_p (pump) surrounding a photovoltaic converter at a temperature T_c in thermal equilibrium with a thermal sink of temperature $T_s = T_c$.

The resulting Landsberg efficiency is

$$\eta_L = 1 - \frac{4}{3}\frac{T_s}{T_p} + \frac{1}{3}\left(\frac{T_s}{T_p}\right)^4 . \tag{2.47}$$

It represents a reversible process of energy conversion (i.e. no generation of entropy), and therefore provides an upper limit of photovoltaic energy conversion efficiency. Landsberg efficiency η_L differs from the efficiency η_C of an idealized Carnot engine (acting between the gas of blackbody radiation at temperature T_p and a converter at temperature $T_c = T_s$)

$$\eta_C = 1 - \frac{T_s}{T_p} \tag{2.48}$$

in that it not only accounts for the entropy of radiation, but also for radiation of the converter. Minor inaccuracies of the Landsberg efficiency limit stem from the fact that it assumes perfect blackbody radiation of both the sun (pump) and the converter. Assuming a converter Temperature of $T_c = T_s = 300\,\text{K}$ and an effective temperature of solar black body radiation of $T_p \approx 5{,}800\,\text{K}$ [9], Carnot efficiency is $\eta_C = 0.948$, whereas Landsberg efficiency is $\eta_L = 0.931$.

Real solar energy conversion features efficiencies below the Landsberg limit. Landsberg efficiency represents the upper efficiency limit of an energy conversion process with respect to the second law of thermodynamics, as any energy conversion process of practical relevance is irreversible (i.e. involves generation of entropy) and accompanied by power losses.

2.4.2 Single Junction-Detailed Balance Limit

In 1961, Shockley and Queisser [10] identified a limit of the solar energy conversion efficiency via semiconductors, which essentially accounts for irreversibility, and which incorporates all loss mechanisms to be outlined in the following. The principle of detailed balance, which requires radiative recombination of a light absorbing semiconductor, sets an upper limit to the maximally achievable electrical power $U_{mpp}I_{mpp}$ of a photovoltaic device exposed to sunlight.

Shockley and Queisser first proposed an idealized calculus, assuming the solar (6,000 K [10]) black body spectrum to be absorbed and to entirely contribute to solar cell current for photon energies above the semiconductor bandgap ε_G, whereas photon energies below ε_G would not be absorbed at all. This calculus yielded an ultimate efficiency limit of $\eta = 0.44$ peaking at a band gap of $\varepsilon_G = 1.1\,\text{eV}$, and suggesting silicon (with a band gap slightly above the latter value) as an optimal single junction photovoltaic device. Accounting for radiative recombination of

absorbed light without any concentration of sunlight, the resulting detailed balance limit encountered at $\varepsilon_G = 1.1$ eV is $\eta = 0.30$.[7]

2.4.3 Classification of Power Losses

One way to classify the power loss mechanisms of a solar cell is to distinguish between thermal, optical, and electrical power losses. The categories overlap to some extent. Yet, this classification proves to be convenient for the specification of the subject of this work.

1. **Thermal** losses denote dissipation of photon energy in excess of a solar cell band gap upon photon absorption. Once excited, electrons and holes quickly relax to the lowest unoccupied states in their respective bands via generation of phonons. In an indirect semiconductor, this relaxation takes place on a timescale much less than excess carrier recombination. Thermal losses imply a major loss mechanism in single-junction devices such as silicon solar cells. They can be reduced via band gap engineering, involving an appropriate design and sequence of materials with different band gaps (e.g. compound semiconductors or quantum wells) tuned to the solar spectrum.
2. **Optical** losses denote deviations from total light absorption by a photovoltaic absorber. They incorporate losses due to reflection, transmission, and parasitic (i.e. non-band-to-band) absorption. High-efficiency solar cells provide miscellaneous concepts to minimize optical power losses, ranging from antireflective coating and light trapping techniques to approaches of up- and/or downconversion of remanent solar irradiation.
3. **Electrical** losses denote losses due to recombination or the imperfection of transport of excess carriers. Recombinative losses involve radiative recombination, recombination due to the interaction among excess carriers (Auger recombination), and recombination at crystal defects and impurities causing electronic states in the band gap (Shockley-Read-Hall (SRH) recombination [11, 12]). In indirect semiconductors, recombinative losses are mostly associated with phonon generation. Thus, they imply thermal losses as well. Transport related loss mechanisms involve resistive losses (finite series resistance of pn-junction device) as well as shunt losses (finite parallel resistance of pn-junction devices accompanied by an ohmic reflow of excess charge).

There is a substantial gap between the above stated detailed balance limit of photovoltaic energy conversion efficiency via single junction devices of $\eta = 0.30$ and the highest efficiencies reached on laboratory type silicon solar cells of $\eta = 0.250 \pm 0.005$ [13–15]. This gap can be attributed to optical and electrical causes. As for

[7] Note that the maximum of the detailed balance limit (without concentration) as a function of band gap energy ε_G is shifted to $\sim$1.3 eV as opposed to the maximum at $\sim$1.1 eV encountered for the ultimate efficiency limit.

optical causes, Shockley and Queisser assumed a Heaviside-like quantum efficiency. In reality, capture of light near the band gap energy ε_G has proven to be among the most demanding challenges on the path toward the Shockley-Queisser-Limit [13]. As for electrical causes, recombination at metal contacts probably represents the most dominant loss mechanism [16, 17].

2.5 Carrier Recombination and Transport

The above-mentioned category of electrical power losses is closely related to both recombination and transport properties of a solar cell. While concepts to adequately and quantitatively describe recombination rates and essential carrier transport properties are detailed in the following chapter, this section is intended to qualitatively sketch the relevance of carrier recombination and transport to solar cell operation.

Upon optical generation of excess electrons and holes in a semiconductor solar cell, excess carriers pile up in the absorber—bringing about a separation of quasi-Fermi levels $\eta_{\sum}$ of electrons and holes equivalent to an implied device voltage $U \approx \frac{\eta_{\sum}}{q}$, which enables the delivery of work $dW = \eta_{\sum} dN$ to an external load by releasing dN carriers of charge q. The steady-state excess carrier density of a solar cell in operation results from a balance between excess carrier generation on the one hand and both excess carrier recombination and charge extraction on the other hand.

2.5.1 Recombination

To some extent, excess charge carrier recombination is inherent to the operation of a semiconductor solar cell. This particularly applies to radiative recombination and Auger recombination. However, SRH recombination through electronic states in the band gap is by no means inherent to solar cell operation. Rather, it largely depends on material quality and on the formation or passivation of electronic states in the band gap during the solar cell production process. Therefore, the prevention and the efficient passivation of such electronic states is the essential task of all solar cell technologists concerned about excess charge carrier recombination.

SRH recombination occurs both at interfaces as well as in the semiconductor bulk. Whereas bulk recombination may be limiting for multicrystalline and possibly upgraded metallurgical grade silicon wafers [18] as well as for p-type materials featuring substantial recombination related to impurity-acceptor complexes [19, 20], the dominant recombination rate of most high efficiency solar cell concepts represents emitter or interface recombination, and particularly recombination at contacts between a semiconductor and metal electrodes [16, 17].

The optimization of the solar cell production process with regard to excess charge carrier recombination calls for accurate and precise measurement techniques of recombination properties, and for an accurate localization of recombination rates in bulk or interfaces.

2.5.2 Transport

Equation 2.38 indicates how electrical charge is delivered to the metal contacts of a solar cell. As can be seen already from this very simple and schematic representation, transport properties such as carrier mobilities, dopant concentrations, and the minority carrier diffusion coefficient largely affect solar cell operation. Therefore, accurate knowledge of these properties is vital for the further improvement of solar cell technologies.

Particularly carrier mobilities in crystalline silicon are often assumed to be accurately known, and as such they are occasionally used in measurements and device simulations as if they featured no uncertainty. Yet, considerable deviations of mobility data and models have been reported in literature (even for monocrystalline silicon) [21–23], and in spite of speculations about potential measurement artifacts, the cause to these deviations has not yet been resolved. With novel techniques to measure both majority and minority carrier mobility, the present work provides new experimental evidence in an unresolved controversy on the one hand. On the other hand, the techniques to be presented open up new pathways to access carrier mobilities in multicrystalline and particularly in upgraded metallurgical grade silicon.

References

1. N.W. Ashcroft, D.N. Mermin, *Solid State Physics* (Saunders College, Philadelphia, 1976)
2. M.A. Green, Intrinsic concentration, effective densities of states, and effective mass in Silicon. J. Appl. Phys. **67**, 2944–2954 (1990)
3. A.B. Sproul, M.A. Green, Improved Value for the Silicon intrinsic carrier concentration from 275 to 375 K. J. Appl. Phys. **70**, 846–854 (1991)
4. A.B. Sproul, M.A. Green, Intrinsic carrier concentration and minority-carrier mobility of Silicon from 77 to 300 K. J. Appl. Phys. **73**, 1214–1225 (1993)
5. P.P. Altermatt, A. Schenk, F. Geelhaar, G. Heiser, Reassessment of the intrinsic carrier density in Crystalline Silicon in view of band-gap narrowing. J. Appl. Phys. **93**, 1598–1604 (2003)
6. P. Würfel, *Physics of Solar Cells: From Basic Principles to Advanced Concepts* (Wiley-VCH, Weinheim, 2009)
7. P.T. Landsberg, G. Tonge, Thermodynamic energy conversion efficiencies. J. Appl. Phys. **51**, R1–R20 (1980)
8. P. Baruch, A. De Vos, P.T. Landsberg, J.E. Parrott, On some thermodynamic aspects of photovoltaic Solar Energy conversion. Solar Energy Mater. Solar Cells **36**, 201–222 (1995)
9. D.R. Williams, Sun Fact Sheet, NASA (2012). http://nssdc.gsfc.nasa.gov/planetary/factsheet/sunfact.html

10. W. Shockley, H.J. Queisser, Detailed balance limit of efficiency of p-n junction solar cells. J. Appl. Phys. **32**, 510–519 (1961)
11. R.N. Hall, Germanium rectifier characteristics. Phys. Rev. **83**, 228 (1951)
12. W. Shockley, W.T. Read, Statistics of the recombinations of holes and electrons. Phys. Rev. **87**, 835–842 (1952)
13. J. Zhao, A. Wang, M.A. Green, F. Ferrazza, 19.8 % efficient "Honeycomb" textured multicrystalline and 24.4 % monocrystalline silicon solar cells. Appl. Phys. Lett. **73**, 1991–1993 (1998)
14. M.A. Green, The path to 25 % silicon solar sell efficiency: history of silicon cell evolution. Prog. Photovoltaics: Res. Appl. **17**, 183–189 (2009)
15. M.A. Green, K. Emery, Y. Hishikawa, W. Warta, E.D. Dunlop, Solar cell efficiency tables (Version 41). Prog. Photovoltaics: Res. Appl. **21**, 1–11 (2012)
16. J. Benick, B. Hoex, M.C.M. Van de Sanden, W.M.M. Kessels, O. Schultz, S.W. Glunz, High efficiency n-type Si solar cells on AlO-passivated Boron Emitters. Appl. Phys. Lett. **92**, 253504 (2008)
17. P.J. Cousins, D.D. Smith, H.C. Luan, J. Manning, T.D. Dennis, A. Waldhauer, K.E. Wilson, G. Harley, W.P. Mulligan, Generation 3: improved performance at lower cost, in *Proceedings of the 35th IEEE PVSC* (Honolulu, 2010), pp. 275–278
18. B. Michl, M. Rüdiger, J.A. Giesecke, M. Hermle, W. Warta, M.C. Schubert, Efficiency limiting bulk recombination in multicrystalline silicon solar cells. Solar Energy Mater. Solar Cells **98**, 441–447 (2012)
19. D. Macdonald, T. Roth, P.N.K. Deenapanray, K. Bothe, P. Pohl, J. Schmidt, Formation rates of Iron-Acceptor pairs in crystalline Silicon. J. Appl. Phys. **98**, 083509 (2005)
20. K. Bothe, J. Schmidt, Electronically activated Boron-Oxygen-related recombination centers in crystalline Silicon. J. Appl. Phys. **99**, 013701 (2006)
21. D.B.M. Klaassen, A unified mobility model for device simulation—I. Model equations and concentration dependence. Solid State Electron. **35**, 953–959 (1992)
22. D.B.M. Klaassen, A unified mobility model for device simulation—II. Temperature dependence of carrier mobility and lifetime. Solid State Electron. **35**, 961–967 (1992)
23. A.B. Sproul, M.A. Green, A.W. Stephens, Accurate determination of minority carrier- and lattice scattering-mobility in Silicon from photoconductance decay. J. Appl. Phys. **72**, 4161–4171 (1992)

http://www.springer.com/978-3-319-06156-6

Quantitative Recombination and Transport Properties in Silicon from Dynamic Luminescence
Giesecke, J.
2014, XXI, 284 p. 86 illus., 63 illus. in color., Hardcover
ISBN: 978-3-319-06156-6